Collecting system–specific deletion of Kcnj10 predisposes for thiazide- and low-potassium diet–induced hypokalemia

Penton, David ; Vohra, Twinkle ; Banki, Eszter ; Wengi, Agnieszka ; Weigert, Maria ; Forst, Anna-Lena ; Bandulik, Sascha ; Warth, Richard ; Loffing, Johannes

Abstract: The basolateral potassium channel KCNJ10 (Kir4.1), is expressed in the renal distal convoluted tubule and controls the activity of the thiazide-sensitive sodium chloride cotransporter. Loss-of-function mutations of KCNJ10 cause EAST/SeSAME syndrome with salt wasting and severe hypokalemia. KCNJ10 is also expressed in the principal cells of the collecting system. However, its pathophysiological role in this segment has not been studied in detail. To address this, we generated the mouse model AQP2cre:Kcnj10flox/flox with a deletion of Kcnj10 specifically in the collecting system (collecting system-Kcnj10-knockout). Collecting system-Kcnj10-knockout mice responded normally to standard and high potassium diet. However, this knockout exhibited a higher kaliuresis and lower plasma potassium than control mice when treated with thiazide diuretics. Likewise, collecting systemKcnj10-knockout displayed an inadequately high kaliuresis and renal sodium retention upon dietary potassium restriction. In this condition, these knockout mice became hypokalemic due to insufficient downregulation of the epithelial sodium channel (ENaC) and the renal outer medullary potassium channel (ROMK) in the collecting system. Consistently, the phenotype of collecting system-Kcnj10-knockout was fully abrogated by ENaC inhibition with amiloride and ameliorated by genetic inactivation of ROMK in the collecting system. Thus, KCNJ10 in the collecting system contributes to the renal control of potassium homeostasis by regulating ENaC and ROMK. Hence, impaired KCNJ10 function in the collecting system predisposes for thiazide and low potassium diet-induced hypokalemia and likely contributes to the pathophysiology of renal potassium loss in EAST/SeSAME syndrome.

DOI: https://doi.org/10.1016/j.kint.2019.12.016

Kcnj10 predisposes for thiazide- and low-potassium diet–induced hypokalemia. Kidney International, 97(6):1208-1218.
DOI: https://doi.org/10.1016/j.kint.2019.12.016

Graphical abstract

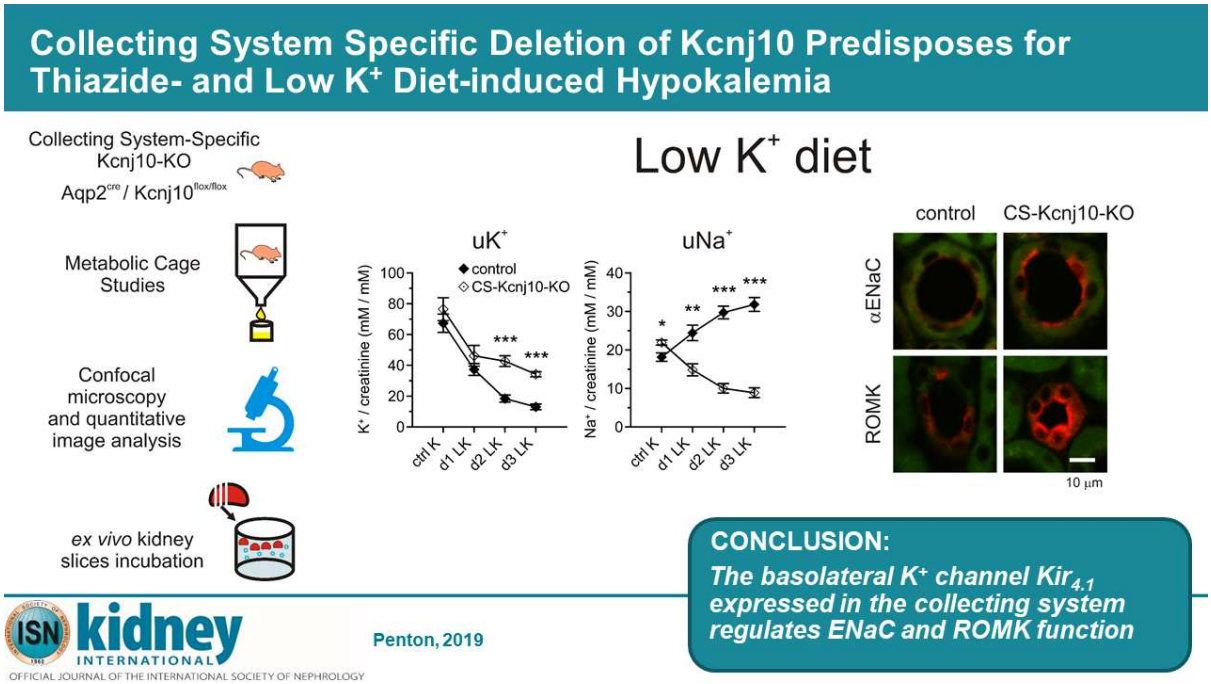

Title

Collecting System Specific Deletion of Kcnj10 Predisposes for Thiazide- and Low K^+ Diet-induced Hypokalemia

David Penton[1,2], Twinkle Vohra[1], Eszter Banki[1,2], Agnieszka Wengi[1], Maria Weigert[3], Anna-Lena Forst[3], Sascha Bandulik[3], Richard Warth[3], Johannes Loffing[1,2]

[1]Institute of Anatomy, University of Zurich, Switzerland, [2]Swiss National Centre for Competence in Research "Kidney Control of Homeostasis", [3]Medical Cell Biology, University of Regensburg, Germany.

RW and JL contributed equally to this study.

Corresponding author*: Johannes Loffing*

Institute of Anatomy, University of Zurich

Winterthurerstrasse 190, CH-8057 Zurich

Switzerland

Phone: +41 (0) 44 635 53 20

Fax: + 41 (0) 44 635 57 02

Email: johannes.loffing@anatomy.uzh.ch

Financial support:

David Penton received support from the European Union's Seventh Framework Program for research, technological development and demonstration under grant agreement no 608847. Richard Warth received support from the "Deutsche Forschungsgemeinschaft" (DFG, German Research Foundation), SFB 699 and SFB 1350, project number 387509280. Johannes Loffing is supported by research funds from the Swiss National Centre for Competence in Research "Kidney.CH", by a project

grant (310030_143929/1) from the Swiss National Science Foundation, and by funds from the Clinical Research Priority Program “HYRENE” of the University of Zurich.

Running title:

Role of $Kir_{4.1}$ in the collecting system

Abstract

The basolateral K^+ channel KCNJ10 ($Kir_{4.1}$), is expressed in the renal distal convoluted tubule (DCT) and controls the activity of the thiazide-sensitive NaCl cotransporter (NCC). Loss-of-function mutations of KCNJ10 cause EAST/SeSAME syndrome with salt wasting and severe hypokalemia. KCNJ10 is also expressed in the principal cells of the collecting system (CS); however, its pathophysiological role in this segment has not been studied in detail. To address this question, we generated the mouse model $AQP2^{cre}$:$Kcnj10^{flox/flox}$ with a deletion of Kcnj10 specifically in the CS (CS-Kcnj10-KO). CS-Kcnj10-KO mice responded normally to standard and high K^+ diet. However, CS-Kcnj10-KO exhibited a higher kaliuresis and lower plasma K^+ than control mice when treated with thiazide diuretics. Likewise, CS-Kcnj10-KO displayed an inadequately high kaliuresis and renal Na^+ retention upon dietary K^+ restriction. In this condition, CS-Kcnj10-KO mice became hypokalemic due to an insufficient downregulation of the epithelial Na^+ channel (ENaC) and the renal outer medullary K^+ channel (ROMK) in the CS. Consistently, the phenotype of CS-Kcnj10-KO was fully abrogated by ENaC inhibition with amiloride and ameliorated by genetic inactivation of ROMK in the CS. In conclusion, KCNJ10 in the CS contributes to the renal control of K^+ homeostasis by regulating ENaC and ROMK. Impaired KCNJ10 function in the CS predisposes for thiazide- and low K^+ diet-induced hypokalemia and likely contributes to the pathophysiology of renal K^+ loss in EAST/SeSAME syndrome.

Keywords:

Potassium homeostasis, diuretics, dietary potassium, collecting duct, connecting tubule, hypokalemia

Translational Statement

The regulation of renal K^+ excretion is crucial for K^+ homeostasis and hence, the proper function of excitable cells. The present study shows that the basolateral K^+ channel $Kir_{4.1}$ (encoded by KCNJ10) acts as a local K^+ sensor in the collecting system. $Kir_{4.1}$ contributes to the aldosterone-independent adaptation of ENaC and ROMK function and hence, K^+ excretion. Mutations and/or polymorphisms of KCNJ10 may contribute to disturbances in K^+ balance.

Introduction

EAST/SeSAME syndrome is caused by loss-of-function mutations of the inwardly rectifying K^+ channel $Kir_{4.1}$ encoded by the KCNJ10 gene[1,2]. This syndrome is characterized by epilepsy, ataxia, sensorineural deafness and a renal salt wasting tubulopathy with severe hypokalemia. In the kidney, KCNJ10 is expressed in the basolateral membrane of the cortical thick ascending limb (TAL), the distal convoluted tubule (DCT) and the principal cells of the collecting system (CS) including the connecting tubule (CNT) and the collecting duct (CD)[3]. $Kir_{4.1}$ may form heterotetramers with $Kir_{5.1}$ (encoded by the Kcnj16 gene), which then set the basolateral membrane voltage of DCT cells[4]. While $Kir_{5.1}$ alone does not conduct measurable K^+ currents[5], $Kir_{4.1}$ functions not only as $Kir_{4.1}/Kir_{5.1}$ heterotetramers but also as $Kir_{4.1}$ homotetramers. It is generally accepted that the renal phenotype in EAST/SeSAME syndrome is a consequence of the defective function of $Kir_{4.1}$ in the DCT, where KCNJ10 expression is at highest levels[6]. Indeed, EAST/SeSAME patients show a renal phenotype that mimics the one seen in patients with Gitelman syndrome who have loss-of-function mutations of the DCT-specific thiazide-sensitive NaCl cotransporter (NCC)[1,7]. Likewise, Kcnj10 knockout mice show a diminished activity of NCC[8].

$Kir_{4.1}$ is thought to interfere with NCC regulation via a complex signaling mechanism that involves the with no lysine kinase WNK4, the STE20/SPS1-related, proline alanine-rich kinase (SPAK) and the oxidative stress responsive kinase 1 (OSR1). Loss of $Kir_{4.1}$ diminishes the plasma membrane voltage of DCT cells, which reduces Cl^- efflux via the basolateral chloride channel ClC-Kb. The subsequently increased intracellular Cl^- concentration inhibits WNK4 and hence reduces SPAK/OSR1-

mediated NCC phosphorylation and activity[9]. The WNK4/SPAK/OSR1 signaling pathway also mediates the K^+ sensitivity of the DCT[10]. Low K^+ increases NCC phosphorylation, while high K^+ rapidly decreases NCC phosphorylation[11,12] via a mechanism that depends on the expression of $Kir_{4.1}$[13].

According to the current concept, K^+-dependent downregulation of NCC increases Na^+ delivery to the CS. In the CS, Na^+ reabsorption via the epithelial Na^+ channel (ENaC) promotes kaliuresis by enhancing the driving force for K^+ excretion via the renal outer medullary K^+ channel (ROMK) and other K^+ channels[14]. High plasma K^+ also stimulates the production of aldosterone by the adrenal gland, which activates ENaC and ROMK in the CS and hence enhances kaliuresis[15]. The combination of NCC inhibition in the DCT with the subsequent aldosterone-dependent activation of Na^+ reabsorption and K^+ secretion in the CS is thought to explain the kaliuresis and hypokalemia observed in patients with genetic (EAST/SeSAME[1] and Gitelman[16] syndromes) or pharmacological (thiazide and thiazide-like diuretics[17]) inactivation of NCC.

Nevertheless, other studies already stressed that NCC inactivation alone is not sufficient to enhance renal K^+ secretion and thus cannot solely explain the kaliuresis upon a high K^+ intake[18]. Likewise, K^+ secretion and activation of ENaC and ROMK in response to dietary K^+ can occur independent from aldosterone[19–21]. Interestingly, *in vivo* data suggests that the CS directly responds to altered plasma K^+[22]. Moreover, previous genetic[23] and pharmacological[24] studies indicated that $Kir_{4.1}$ participates also in setting the membrane potential of principal cells in the CS. Therefore, we hypothesized that $Kir_{4.1}$ may act as a local K^+ sensor in the CS to mediate the adaptation of ENaC and ROMK to dietary K^+. Loss of $Kir_{4.1}$ in the CS could lead to a

maladaptation of ENaC and ROMK and contribute to the hypokalemia in EAST/SeSAME patients.

Results

CS-Kcnj10-KO mice do not exhibit any evident clinical phenotype under standard conditions.

To investigate the function of $Kir_{4.1}$ in the CNT and CD, collecting system (CS)-specific Kcnj10-KO mice (CS-Kcnj10-KO) were generated by breeding mice with ´floxed´ Kcnj10 alleles ($Kcnj10^{flox/flox}$) with mice expressing the Cre recombinase under the control of the Aqp2 promoter ($Aqp2^{cre}$). CS-Kcnj10-KO mice were born in a Mendelian ratio and thrived normally. Immunofluorescence staining of consecutive kidney sections with antibodies against AQP2, $Kir_{4.1}$ and NCC confirmed that control mice express $Kir_{4.1}$ in both NCC-positive DCTs and AQP2-positive CS. In CS-Kcnj10-KO mice, the expression of $Kir_{4.1}$ in DCTs was unaffected, while it was completely absent in the CS (Figs. 1 A and B). Under standard diet, the plasma parameters of CS-Kcnj10-KO mice were similar to those of control mice (Table 1). Consistent with a normal Na^+ and K^+ balance under control conditions, renal renin mRNA and plasma aldosterone concentration were similar in control and CS-Kcnj10-KO mice (Fig. 1C). Furthermore, abundances and post-translational modifications (cleavage, glycosylation and phosphorylation) of channels and transporters in the renal tubule (e.g. NCC, ENaC, ROMK, Na^+/K^+ - ATPase and AQP2) were similar in both genotypes (Figs. 1 D and E).

The potassium sensitivity of the DCT is preserved in CS-Kcnj10-KO mice.

An acute rise of plasma or extracellular K^+ promotes a rapid dephosphorylation of NCC [11,12,10,25], which is thought to depend on Kcnj10[26]. To test if K^+-dependent regulation

of NCC in CS-Kcnj10-KO mice is affected, kidney slices were incubated ex vivo with different extracellular K^+ concentrations. As shown in Figs. 2 A and B, a high extracellular K^+ concentration decreased while a low extracellular K^+ concentration increased NCC phosphorylation in similar ways in both genotypes. In kidney slices from CS-Kcnj10-KO incubated with 3-5 mmol/L of K^+, the phosphorylation of NCC was slightly increased. The cause of this slight difference is unclear; nevertheless, CS-Kcnj10-KO and control animals exhibited similar plasma K^+ and NCC phosphorylation levels *in vivo* under standard diet (Fig. 1D). Moreover, the inverse correlation between NCC phosphorylation and plasma K^+ concentration was similar for control and CS-Kcnj10-KO mice (Supplementary figure 1).

CS-Kcnj10-KO mice are prone to develop thiazide-induced hypokalemia.

Loss of function of $Kir_{4.1}$ causes hypokalemia in patients with EAST/SeSAME syndrome and in Kcnj10-KO mouse models[1,13] and is thought to be related to a malfunction of the DCT[6,8,13]. In line with this hypothesis, CS-Kcnj10-KO mice are not hypokalemic under standard conditions. When treated with HCTZ, control and CS-Kcnj10-KO mice exhibited a similar natriuresis (Fig. 3 A and B), consistent with similar NCC abundances in both genotypes. Compared to the time d0 (before thiazide-treatment), control animals did not display a significant HCTZ-induced kaliuresis as previously described[18] (Fig. 3 A and B). On the contrary, CS-Kcnj10-KO animals exhibited an increased kaliuresis and urinary K^+/Na^+ ratio, (Fig. 3 A and B). Consequently, after three days of continuous thiazide-treatment, CS-Kcnj10-KO had significantly lower plasma K^+ concentrations than control mice and developed

hypochloremic metabolic alkalosis and hyponatremia (Table 2), recapitulating the main symptoms observed in EAST/SeSAME patients.

CS-Kcnj10-KO mice develop severe hypokalemia upon dietary K^+ restriction.

Mouse neonates with a global Kcnj10 deletion have depolarized principal cells in the CS and an increased ENaC expression despite of hypokalemia[23]. Now, we tested whether the lack of $Kir_{4.1}$ in the CS directly stimulates ENaC and activates K^+ excretion. To test this hypothesis, CS-Kcnj10-KO and control mice were fed a low K^+ diet (<0.05% K^+) for three days and urinary and plasma parameters were assessed.

While control animals immediately started losing Na^+, CS-Kcnj10-KO mice retained Na^+ under low dietary K^+ conditions (Fig. 4A). Moreover, after the second day on a low K^+ diet, CS-Kcnj10-KO mice exhibited an inappropriately high kaliuresis compared to control animals. Consequently, CS-Kcnj10-KO mice developed severe hypokalemia and hypochloremia (Table 3). In contrast to the maladaptation on low K^+ diet, CS-Kcnj10-KO mice adapted normally to a dietary K^+ load (Fig. 4B). (Table 4).

CS-Kcnj10-KO mice fail to inactivate ENaC when fed a low K^+ diet.

Next, we studied the abundance of distal tubule ion channels and transporters in control and CS-Kcnj10-KO mice subjected to dietary K^+ deprivation. As shown in Fig. 5A and B, NCC phosphorylation was significantly increased in CS-Kcnj10-KO compared to control mice, likely reflecting the more severe hypokalemia of CS-Kcnj10-KO. Moreover, α-ENaC cleavage was significantly augmented in CS-Kcnj10-KO despite the severe hypokalemia.

To study the expression and localization of αENaC at the tubular level, we performed immunofluorescence stainings on kidneys from control and CS-Kcnj10-KO mice after 3 days of dietary K^+ deprivation. As shown in Fig. 5C, the apical localization of αENaC was increased in AQP2-positive CS of CS-Kcnj10-KO mice compared to control animals. To evaluate the functional significance of the inappropriate high apical ENaC abundance in the CS of CS-Kcnj10-KO mice, CS-Kcnj10-KO and control animals were kept on a low K^+ diet for two days in metabolic cages. Afterwards, a single i.p. injection of the ENaC inhibitor amiloride was administered and urine was collected for the next 4h. Consistent with a low K^+ diet-induced ENaC inactivation, control mice did not reveal a significant natriuresis and kaliuresis in response to amiloride. In contrast, CS-Kcnj10-KO mice showed a pronounced amiloride-induced natriuresis and kaliuresis (Fig. 5D).

CS-Kcnj10-KO mice fail to inactivate ROMK when fed a low K^+ diet.

As shown in Fig. 1D and Fig. 5A, the expression and glycosylation of ROMK in the whole kidney was unchanged in CS-Kcnj10-KO mice compared to control mice. However, ROMK is not only expressed in the CS, but highly abundant in the thick ascending limb (TAL) and in the DCT[27] which could mask subtle changes in the abundance of ROMK in the CS. To study the expression and localization of ROMK specifically in the CS, we performed immunofluorescent studies on consecutive sections of kidneys from control and CS-Kcnj10-KO mice upon 3 days of dietary K^+ deprivation. As shown in Fig. 6A, the abundance of ROMK in the AQP2-positive CS of control animals was very weak compared to the AQP2-negative TAL cells. However, in the CS-Kcnj10-KO mice, ROMK abundance was profoundly increased in the apical region of the principal cells in the CS cells and reached a staining intensity quite similar

to the one seen in the TAL cells. Quantification of ROMK staining intensities across the axis (basal to apical) of CS cells from control and CS-Kcnj10-KO confirmed the visual observations (Fig. 6A).

To assess the contribution of the inappropriate regulation of ROMK to the phenotype of CS-Kcnj10-KO mice, Kcnj1 (ROMK) was genetically ablated in the CS of CS-Kcnj10-KO mice. To this end, CS-Kcnj10-KO mice were crossed with a newly developed $Kcnj1^{flox/flox}$ mouse line to obtain a CS-specific Kcnj10 and ROMK double-KO (CS-Kcnj10-ROMK-KO) (Supplementary Figure 2). Apart from a mild hypercalciuria, the CS-Kcnj10-ROMK-KO mice were normal under control conditions (Supplementary Table 1). When subjected to a low K^+ diet for 3 days, the CS-Kcnj10-ROMK-KO were protected from the severe hypokalemia observed in CS-Kcnj10-KO mice and had plasma K^+ levels in the range of control mice (Fig. 6B and Table 5). Consistent with the measured plasma K^+ levels, the renal K^+ loss of CS-Kcnj10-ROMK-KO mice on day 2 of dietary K^+ deprivation was significantly lower than the one seen in CS-Kcnj10-KO mice (21.0 ± 2.2 (n=9) vs. 54.3 ± 6.5 (n=6); $p<0.0001$; unpaired Students t-test). Nevertheless, despite the deletion of ROMK, CS-Kcnj10-ROMK-KO mice excreted significantly more K^+ in the urine than control animals (Fig. 6C, open circles). Interestingly, ENaC inhibiton by amiloride significantly reduced urinary K^+ excretion, but had little effect on urinary Na^+ excretion in CS-Kcnj10-ROMK-KO mice. The reason for the reduced amiloride response in double KO mice compared with the single CS-Kcnj10-KO mice is unclear, but may indicate that the loss of ROMK affects also ENaC activity. Future studies will have to address this intriguing possibility.

Discussion

EAST/SeSAME patients suffer from loss-of-function mutations of KCNJ10 in the DCT and display severe hypokalemia and a renal tubulopathy that is reminiscent of Gitelman's syndrome[1–3]. These observations led to the current concept that the renal phenotype of patients with loss-of-function mutations in KCNJ10 is mainly due to an impaired DCT function[3]. According to this concept, the reduced NCC activity in patients with EAST/SeSAME syndrome results in an increased NaCl delivery to the CS. The concomitant enhanced Na^+ reabsorption in the principal cells of the CS via ENaC leads to an increased K^+ secretion via ROMK resulting in hypokalemia. This situation is further aggravated by an activation of the renin-angiotensin-aldosterone and the concurrent enhancement of ENaC function. In fact, mouse models with global or kidney-specific deletion of Kcnj10 showed a strong downregulation of NCC[8,13] and an up-regulation of ENaC[23], which is thought to explain the severe hypokalemia observed in these mice. Now, we used a mouse model with a targeted deletion of Kcnj10 specifically in the principal cells of the CS to test the hypothesis that KCNJ10 participates to the direct regulation of ENaC and ROMK and that a lack of KCNJ10 in the CS contributes to the hypokalemia.

In contrast to total or kidney-specific Kcnj10-KO mice, CS-Kcnj10-KO mice had an intact DCT function and did not show an apparent phenotype under control conditions. The DCT of CS-Kcnj10-KO mice exhibited a preserved sensitivity to changes in extracellular K^+ as evidenced by the K^+-dependency of NCC phosphorylation *in vivo and ex vivo*. Moreover, CS-Kcnj10-KO mice revealed a normal adaptation to increased dietary intake of K^+. However, when placed on a low K^+ diet, the CS-Kcnj10-KO mice became severely hypokalemic. Likewise, CS-Kcnj10-KO mice developed hypokalemia

and hypochloremic metabolic alkalosis when treated with the NCC inhibitor HCTZ, recapitulating the main renal symptoms of EAST/SeSAME syndrome[1]. These findings support the idea that the renal phenotype in EAST/SeSAME syndrome results from the combined defect of NCC regulation in the DCT and ENaC and ROMK regulation in the CS.

The secretion of K^+ in the CS is thought to be mediated via an aldosterone-dependent upregulation of ENaC[28,29] and the activation of ROMK[27] and the large K^+ conductance (BK) potassium channels[30,31]. In addition, an aldosterone-independent control of renal K^+ secretion was suggested[32], which might involve a kaliuretic factor [33 34]. However, the nature and identity of this kaliuretic factor remains elusive. Recently, $Kir_{4.1}$, in combination with $Kir_{5.1}$[24], was proposed to act as a K^+ sensor in the DCT[13] that directly mediates the regulation of NCC activity via dietary K^+[26] and Na^+[35]. Now, our data suggest that $Kir_{4.1}$ does also act as a local K^+ sensor in the CS and directly adapts the K^+ secretion of the CS to altered extracellular K^+ concentrations. Interestingly, also Dahl salt-sensitive rats deficient for Kcnj16 ($SS^{Kcnj16-/-}$) develop severe, life-threatening hypokalemia when placed on a high NaCl diet[36]. The phenotype was rescued by the ENaC inhibitor benzamil suggesting that $Kir_{5.1}$ also participates to the direct adaptation of ENaC function to altered dietary ion intakes.

Previous studies indicated that the activity of ENaC and ROMK in the CS correlates with the extent of the proteolytic cleavage of the αENaC subunits[37] and their apical localization[27]. Our immunoblot data on kidney lysates together with our immunofluorescence studies indicate that the CS-Kcnj10-KO have an inappropriately high ENaC and ROMK activity on a low K^+ diet, which likely explains the renal K^+ loss and severe hypokalemia seen in these mice. Consistent with this idea and in agreement with the experiments by Palygin and coworkers in $SS^{Kcnj16-/-}$ rats[36], the

pharmacological inhibition of ENaC by amiloride fully abrogated the urinary K^+ loss in CS-Kcnj10-KO mice. Moreover, the genetic inactivation of ROMK significantly mitigated the renal K^+ loss. However, we observed a slight, but persistent renal loss of K^+ in CS-Kcnj10-ROMK-KO suggesting that additional K^+ channels (e.g. BK) contribute to the inappropriately high K^+ secretion of CS-Kcnj10-KO mice on a low K^+ diet. Indeed, previous studies suggested that both ROMK and BK contribute to renal K^+ excretion and that each channel can compensate for the lack of the other one[38]. Thus, our data indicate that Kcnj10 contributes to the direct K^+-dependent regulation of ENaC, ROMK and probably other K^+ channels in the CS. As such, our data are compatible with previous studies suggesting that dietary K^+ directly regulates the activity of ENaC and ROMK[20,22,39], which occurs independent from aldosterone[21].

While $Kir_{4.1}$ regulates NCC activity via WNK/SPAK pathway[13], the molecular mechanisms mediating the regulation of ENaC and ROMK expression in the CS are unclear. The kidney-specific WNK1 (KS-WNK1)[40] and the mTORC2[41] pathway were implicated in the regulation of ROMK and in the control of renal K^+ excretion. Likewise, the serum- and glucocorticoid-induced kinase 1 (SGK1), and the glucocorticoid-induced leucine zipper protein (GILZ1) were suggested to synergistically control ENaC cell surface expression and activity[42]. While this manuscript was submitted, Sorensen and coworkers reported that extracellular K^+ directly stimulates the mTORC2-dependent phosphorylation of SGK1 in cultured CCD cells which activates ENaC and hence favors K^+ secretion[43]. Pharmacological inhibition of $Kir_{4.1}$ with the inhibitor VU0134992[44] blocked the activation of mTORC2 and ENaC suggesting an involvement of $Kir_{4.1}$ in the K^+-dependent regulation of ENaC. Using a genetic approach, our current study demonstrates that $Kir_{4.1}$ is indeed critical for a proper downregulation of both ENaC and ROMK in response to a low K^+ diet *in vivo*.

Role of $Kir_{4.1}$ in the collecting system

In summary, our data demonstrate that the $Kir_{4.1}$ in the CS is indispensable for the proper renal adaptation to dietary K^+ depletion and modulates the response to thiazide diuretics. Our study suggests that the severe hypokalemia in EAST/SeSAME patients is not only explained by a downregulation of Na^+ transport in the DCT and an aldosterone-dependent upregulation of K^+ excretion in the CS. The hypokalemia is likely related also to a disturbed K^+-sensing in the CS that impairs the appropriate adaptation of ENaC and ROMK activity to low plasma K^+ levels (Fig. 7). Interestingly, several single nucleotide polymorphisms (SNPs) that change the biophysical properties of $Kir_{4.1}$ have been described in the KCNJ10 gene[45]. It is tempting to speculate that other unexplained variants of hypokalemia might be linked to polymorphisms in Kcnj10 / Kcnj16 or other molecular players involved in the direct adaptation of ENaC and ROMK function to altered plasma K^+ concentrations.

Methods

Animals

Mice were maintained at a 12/12 h light/dark cycle with access to standard chow (3430 Kliba-Nafag, Kaiseraugst, Switzerland) and water ad libitum. Animal experiments were conducted according to Swiss Laws and approved by the veterinary administration of the Canton of Zurich, Switzerland (License numbers: 213/2015, and 135/2018). For each experimental series, animals with matching weight, sex and age were used. CS-Kcnj10-KO mice were generated by cross-breeding $Kir_{4.1}^{f/f}$ (Jackson Laboratories Stock No: 026826)[46] with the CS-specific Cre mouse line Aquaporin 2 (AQP2)-Cre[47]. Additionally, mice with the exon 2 of Kcnj1 (ROMK) flanked by *loxP* sites were custom-generated by OZgene (Bentley DC, WA 6983, Australia) (Supplementary Fig. 2). The CS-Kcnj10-ROMK-KO mouse line was generated by cross breeding CS-Kcnj10-KO mice with $Kcnj1^{f/f}$ mice (Supplementary Fig. 2). Mice CS-Kcnj10-KO and CS-Kcnj10-ROMK-KO were kept homozygous for the floxed alleles and heterozygous for the expression of the cre-recombinase. Littermates carrying only the floxed alleles and not expressing the cre recombinase were used as control.

Diets

Potassium deficient (Low K^+; K^+ content < 0.05%, Na^+ content 0.22%) and the correspondent control diet (ctrl K^+; K^+ content = 0.97%, Na^+ content 0.21%) were purchased from Ssniff Spezialdiaeten (Soest, Germany Cat No: E15450-20 and E15000-00 respectively). For the high K^+ diet described in Fig. 4B, 100g of standard chow (3430 Kliba-Nafag, Kaiseraugst, Switzerland) with a K^+ content of 0.78% (Na^+ content 0.2 %) was minced and mixed with 4.2g of KCl to obtain a K^+ content of 3%

(High K^+ diet). The powdered food was given as a paste by mixing the same amount (weight : weight) of powdered food and water. As control, the same preparation without KCl addition was used.

Metabolic cages studies

Mice were adapted to metabolic cages (Techniplast, Buguggiate, Varese, Italy) for two days on control diet. Afterwards, the diet was changed to either low K^+ or high K^+ during 3 days. 24h urine was collected and frozen. After 3 days with the experimental diet, animals were sacrificed by terminal exsanguination via the abdominal vena cava and blood and kidney samples were collected. Urine ion analysis was performed by flame photometry (Eppendorf, EFOX 5053, Burladingen, Germany). Urinary creatinine was quantified using the Jaffe method[48].

Antibodies

We used previously generated and described antibodies against (dilution used for immunoblots (IB) and Immunofluorescence (IF) are indicated in parenthesis) tNCC[11] (IB: 1:2500, IF: 1:10000), pT53NCC[11] (IB: 1:2500), α-ENaC[11] (IB: 1:5000, IF: 1:20000), β-ENaC[49] (IB: 1:10000), γ-ENaC[49] (IB: 1:10000) and AQP2[49] (IB: 1:20000, IF 1:200000) . The antibody against $Kir_{4.1}$ was from Alomone Laboratories (Jerusalem, Israel, Cat No: APC-035) (IF: 1:10000). The antibody against β-actin was from Sigma Aldrich (Sigma, Buchs, Switzerland Cat. No: A5316) (IB: 1:5000). The antibody against Na/K-ATPase was a kind gift from Dr. Eric Féraille[50] (IB: 1:10000). A novel rabbit anti-ROMK antibody was generated as described in the supplement and used for IB and IF at dilutions of 1: 2000 and 1: 12000, respectively.

Hydrochlorothiazide treatment

Mice were adapted to metabolic cages for 2 days under control diet (3430 Kliba-Nafag, Kaiseraugst, Switzerland) minced and mixed with water (weight : weight). On the third day, the diet was mixed with hydrochlorothiazide (HCTZ) (Sigma, Buchs, Switzerland. Cat. No: H4759) to achieve 40mg of HCTZ /kg of body weight ingested per day. The treatment had a duration of three days. The amount of HCTZ added to the food was calculated each day taking into account the average food intake of the previous day. There were no differences in food ingestion between genotypes.

Amiloride test

Mice were adapted to metabolic cages as previously described and received a low K^+ diet during two consecutive days. Base line urine samples were collected in the morning after the second experimental day. Afterwards, each mouse received a single intraperitoneal dose of 5 μg of amiloride / gram of body weight. Amiloride (Alomone Laboratories, Jerusalem, Israel, Cat No: A-140) was diluted in 0.9% sterile NaCl solution in a final concentration of 0.5 mg/mL. Each animal received 10 μL of this solution per gram of body weight. Animals were kept in the metabolic cages for the next 4 hours and the urine corresponding to this time was collected and analyzed.

Blood sample collection and analysis

Blood samples were collected under Isoflurane anesthesia (Attane, Piramal, India) from the inferior vena cava. Blood analysis was immediately performed using the Blood Gas analyzer (ABL80 FLEX, Radiometer, Denmark). The remaining blood was centrifuged and the plasma was frozen for further analysis. Plasma aldosterone levels

were measured using a commercially available Aldosterone ELISA Kit (Caymann Chemical, USA) and following the manufacturer instructions.

Kidney slices and Immunoblotting

Kidney slice preparation and immunoblotting were previously described elsewhere[12]. In all immunoblots presented in this manuscript, both control and experimental groups were run on the same gel. The dashed line in Figs. 1D and 5A were included to help readers to easily identify the bands belonging to each group, but do not indicate that the samples were run on separate gels. For the densitometric analysis included in Figs. 1 and 5 the bands were first normalized to the loading control (β-actin) and then to the average of control group.

Immunofluorescence (IF) and IF quantification

Immunofluorescence (IF) and IF quantification was performed as described in the supplement.

Statistics

Unpaired student's t-test was used to compare between two groups. Shapiro-Wilk normality test was used to analyze the normal distribution of the samples. For multiple comparison, one-way ANOVA or two-way ANOVA with Tukey multiple comparison post-test were performed using the software GraphPad Prism 8 (GraphPad Software, San Diego, California, USA).

Disclosure

None

Acknowledgments

The authors thank Monique Carrel, Ines Tegtmeier, Pascal Peretti and Michèle Heidemeyer for excellent technical assistance. The authors also the Center of Microscopy and Image Analysis (ZMB) from the University of Zurich, and particularly Dr. Joana R. Martins, for excellent support with confocal microscopy and image analysis. Authors are thankful to Dr. Carsten Wagner (University of Zurich, Switzerland) and Dr. Markus Bleich (University of Kiel, Germany) for fruitful discussions. Part of this study was presented at the Annual Meeting of the American Society of Nephrology 2019 in Washington, DC.

Supplementary Material

The following supplementary information is available on Kidney International's website

- Supplementary Methods
- Supplementary Figure 1
- Supplementary Figure 2
- Supplementary Figure 3
- Supplementary Figure 4
- Supplementary Table 1
- Supplementary Macro

References

1. Bockenhauer D, Feather S, Stanescu HC *et al.* Epilepsy, ataxia, sensorineural deafness, tubulopathy, and KCNJ10 mutations. *N. Engl. J. Med.* 2009; **360**: 1960–70.

2. Scholl UI, Choi M, Liu T *et al.* Seizures, sensorineural deafness, ataxia, mental retardation, and electrolyte imbalance (SeSAME syndrome) caused by mutations in KCNJ10. *Proc. Natl. Acad. Sci. U. S. A.* 2009; **106**: 5842–7.

3. Reichold M, Zdebik AA, Lieberer E *et al.* KCNJ10 gene mutations causing EAST syndrome (epilepsy, ataxia, sensorineural deafness, and tubulopathy) disrupt channel function. *Proc. Natl. Acad. Sci. U. S. A.* 2010; **107**: 14490–5.

4. Palygin O, Pochynyuk O, Staruschenko A. Distal tubule basolateral potassium channels: cellular and molecular mechanisms of regulation. *Curr. Opin. Nephrol. Hypertens.* 2018; **27**: 373–378.

5. Bond CT, Pessia M, Xia XM *et al.* Cloning and expression of a family of inward rectifier potassium channels. *Receptors Channels* 1994; **2**: 183–91.

6. Scholl UI, Dave HB, Lu M *et al.* SeSAME/EAST syndrome--phenotypic variability and delayed activity of the distal convoluted tubule. *Pediatr. Nephrol.* 2012; **27**: 2081–2090.

7. Simon DB, Nelson-Williams C, Bia MJ *et al.* Gitelman's variant of Bartter's syndrome, inherited hypokalaemic alkalosis, is caused by mutations in the thiazide-sensitive Na-Cl cotransporter. *Nat. Genet.* 1996; **12**: 24–30.

8. Zhang C, Wang L, Zhang J *et al.* KCNJ10 determines the expression of the apical Na-Cl cotransporter (NCC) in the early distal convoluted tubule (DCT1). *Proc. Natl. Acad. Sci. U. S. A.* 2014; **111**: 11864–9.

9. Wang W-H. Basolateral Kir4.1 activity in the distal convoluted tubule regulates K secretion by determining NaCl cotransporter activity. *Curr. Opin. Nephrol. Hypertens.* 2016; **25**: 429–35.

10. Terker ASS, Zhang CCC, McCormick JA a *et al.* Potassium Modulates Electrolyte Balance and Blood Pressure through Effects on Distal Cell Voltage and Chloride. *Cell Metab.* 2015; **21**: 39–50.

11. Sorensen M V, Grossmann S, Roesinger M *et al.* Rapid dephosphorylation of the renal sodium chloride cotransporter in response to oral potassium intake in mice. *Kidney Int.* 2013; **83**: 811–24.

12. Penton D, Czogalla J, Wengi A *et al.* Extracellular K(+) rapidly controls NaCl cotransporter phosphorylation in the native distal convoluted tubule by Cl(-) -dependent and independent mechanisms. *J. Physiol.* 2016; **594**: 6319–6331.

13. Cuevas CA, Su X-T, Wang M-X *et al.* Potassium Sensing by Renal Distal Tubules Requires Kir4.1. *J. Am. Soc. Nephrol.* 2017; **28**: 1814–1825.

14. McDonough AA, Youn JH. Need to quickly excrete K+? Turn off NCC. *Kidney Int.* 2013; **83**: 779–782.

15. Penton D, Czogalla J, Loffing J. Dietary potassium and the renal control of salt balance and blood pressure. *Pflügers Arch. Eur. J. Physiol.* 2015; **467**: 513–30.

16. Gitelman HJ, Graham JB, Welt LG. A new familial disorder characterized by hypokalemia and hypomagnesemia. *Trans. Assoc. Am. Physicians* 1966; **79**: 221–35.

17. Ellison DH, Loffing J. Thiazide effects and adverse effects: Insights from molecular genetics. *Hypertension* 2009; **54**: 196–202.

18. Hunter RW, Craigie E, Homer NZM *et al.* Acute inhibition of NCC does not activate distal electrogenic Na+ reabsorption or kaliuresis. *Am. J. Physiol. Renal Physiol.* 2014; **306**: F457-67.

19. Stanton B, Pan L, Deetjen H *et al.* Independent effects of aldosterone and potassium on induction of potassium adaptation in rat kidney. *J. Clin. Invest.* 1987; **79**: 198–206.

20. Palmer LG, Frindt G. Aldosterone and potassium secretion by the cortical collecting duct. *Kidney Int.* 2000; **57**: 1324–1328.

21. Todkar A, Picard N, Loffing-Cueni D *et al.* Mechanisms of Renal Control of Potassium Homeostasis in Complete Aldosterone Deficiency. *J. Am. Soc. Nephrol.* 2014: 1–14.

22. Wingo CS, Seldin DW, Kokko JP *et al.* Dietary modulation of active potassium secretion in the cortical collecting tubule of adrenalectomized rabbits. *J. Clin. Invest.* 1982; **70**: 579–86.

23. Su X-T, Zhang C, Wang L *et al.* Disruption of KCNJ10 (Kir4.1) stimulates the expression of ENaC in the collecting duct. *Am. J. Physiol. Renal Physiol.* 2016; **310**: F985-93.

24. Palygin O, Pochynyuk O, Staruschenko A. Role and mechanisms of regulation of the basolateral Kir 4.1/Kir 5.1 K(+) channels in the distal tubules. *Acta Physiol. (Oxf).* 2016: 1–14.

25. Rengarajan S, Lee DH, Oh YT *et al.* Increasing plasma [K+] by intravenous potassium infusion reduces NCC phosphorylation and drives kaliuresis and natriuresis. *Am. J. Physiol. Renal Physiol.* 2014; **306**: F1059-68.

26. Wang M-X, Cuevas CA, Su X-T *et al.* Potassium intake modulates the thiazide-sensitive sodium-chloride cotransporter (NCC) activity via the Kir4.1 potassium channel. *Kidney Int.* 2017: 1–10.

27. Wade JB, Fang L, Coleman R a *et al.* Differential regulation of ROMK (Kir1.1) in distal nephron segments by dietary potassium. *Am. J. Physiol. Renal Physiol.* 2011; **300**: F1385-93.

28. Pácha J, Frindt G, Antonian L *et al.* Regulation of Na channels of the rat cortical collecting tubule by aldosterone. *J. Gen. Physiol.* 1993; **102**: 25–42.

29. Stokes JB. Mineralocorticoid effect on K+ permeability of the rabbit cortical collecting tubule. *Kidney Int.* 1985; **28**: 640–5.

30. Satlin LM, Carattino MD, Liu W *et al.* Regulation of cation transport in the distal nephron by mechanical forces. *Am. J. Physiol. Physiol.* 2006; **291**: F923–F931.

31. Bailey MA, Cantone A, Yan Q *et al.* Maxi-K channels contribute to urinary potassium excretion in the ROMK-deficient mouse model of Type II Bartter's syndrome and in adaptation to a high-K diet. *Kidney Int.* 2006; **70**: 51–59.

32. McDonough AA, Youn JH. Potassium Homeostasis: The Knowns, the Unknowns, and the Health Benefits. *Physiology* 2017; **32**: 100–111.

33. Rabinowitz L. Aldosterone and potassium homeostasis. *Kidney Int.* 1996; **49**: 1738–1742.

34. Preston RA, Afshartous D, Rodco R *et al.* Evidence for a gastrointestinal–renal kaliuretic signaling axis in humans. *Kidney Int.* 2015; **88**: 1383–1391.

35. Wu P, Gao Z-X, Su X-T *et al.* Kir4.1/Kir5.1 Activity Is Essential for Dietary Sodium Intake-Induced Modulation of Na-Cl Cotransporter. *J. Am. Soc. Nephrol.* 2019; **30**: 216–227.

36. Palygin O, Levchenko V, Ilatovskaya D V *et al.* Essential role of Kir5.1 channels in renal salt handling and blood pressure control. *JCI insight* 2017; **2**: 1–16.

37. Bhalla V, Hallows KR. Mechanisms of ENaC Regulation and Clinical Implications. *J. Am. Soc. Nephrol.* 2008; **19**: 1845–1854.

38. Sansom SC, Welling PA. Two channels for one job. *Kidney Int.* 2007; **72**: 529–530.

39. Palmer LG, Antonian L, Frindt G. Regulation of apical K and Na channels and Na/K pumps in rat cortical collecting tubule by dietary K. *J. Gen. Physiol.* 1994; **104**: 693–710.

40. Gao Z-X, Wu P, Hadchouel J *et al.* Role of WNK4 and kidney-specific WNK1 in mediating the effect of high dietary K + intake on ROMK channel in the distal convoluted tubule . *Am. J. Physiol. Physiol.* 2018; **315**: F223–F230.

41. Grahammer F, Nesterov V, Ahmed A *et al.* Mtorc2 critically regulates renal potassium handling. *J. Clin. Invest.* 2016; **126**: 1773–1782.

42. Soundararajan R, Melters D, Shih I-C *et al.* Epithelial sodium channel regulated by differential composition of a signaling complex. *Proc. Natl. Acad. Sci. U. S. A.* 2009; **106**: 7804–9.

43. Sørensen MV, Saha B, Jensen IS *et al.* Potassium acts through mTOR to regulate its own secretion. *JCI insight* 2019; **5**.

44. Kharade S V., Kurata H, Bender AM *et al.* Discovery, characterization, and effects on renal fluid and electrolyte excretion of the Kir4.1 potassium channel pore blocker, VU0134992. *Mol. Pharmacol.* 2018; **94**: 926–937.

45. Méndez-González MP, Kucheryavykh Y V., Zayas-Santiago A *et al.* Novel KCNJ10 gene variations compromise function of inwardly rectifying potassium channel 4.1. *J. Biol. Chem.* 2016; **291**: 7716–7726.

46. Djukic B, Casper KB, Philpot BD *et al.* Conditional knock-out of Kir4.1 leads to glial membrane depolarization, inhibition of potassium and glutamate uptake, and enhanced short-term synaptic potentiation. *J. Neurosci.* 2007; **27**: 11354–11365.

47. Ronzaud C, Loffing J, Bleich M *et al.* Impairment of sodium balance in mice deficient in renal principal cell mineralocorticoid receptor. *J. Am. Soc. Nephrol.* 2007; **18**: 1679–1687.

48. Seaton B, Ali A. Simplified manual high performance clinical chemistry methods for developing countries. *Med. Lab. Sci.* 1984; **41**: 327–36.

49. Wagner CA, Loffing-Cueni D, Yan Q *et al.* Mouse model of type II Bartter's syndrome. II.

Altered expression of renal sodium- and water-transporting proteins. *Am. J. Physiol. Renal Physiol.* 2008; **294**: F1373-80.

50. Carranza ML, Féraille E, Favre H. Protein kinase C-dependent phosphorylation of Na(+)-K(+)-ATPase alpha-subunit in rat kidney cortical tubules. *Am. J. Physiol.* 1996; **271**: C136-43.

Figure 1: Characterization of CS-Kcnj10-KO mice under standard conditions. **A:** Representative immunofluorescence staining of consecutive sections of kidneys from control and CS-Kcnj10-KOmice. Sections were stained with the DCT marker NCC (labelled with a D in the middle image), $Kir_{4.1}$ and the CS marker AQP2 (labeled with a star in the middle image). Scale bar 50 μm **B:** Quantification of immunofluorescence staining of $Kir_{4.1}$ in sections from control (n=6) and CS-Kcnj10-KO (n=5) mice. In red, the mean fluorescence intensity of proximal tubules (negative for $Kir_{4.1}$) is represented. **C:** Quantification of renin gene expression by qRT-PCR (left graph) and plasma aldosterone concentrations (right graph) in CS-Kcnj10-KO and control mice (n=5 mice per genotype). Horizontal lines represent the mean of each group. **D:** Immunoblot of the main channels and transporters expressed in the distal nephron of CS-Kcnj10-KO and control mice. Molecular weights indicated on the right in kDa. **E:** Densitometric analysis of immunoblots in D normalized to control (in red). In the whole figure statistical differences assessed by unpaired Student's t-test (ns non-significant; *** $p<0.001$).

Figure 2: Potassium sensitivity of DCT in control and CS-Kcnj10-KO mice **A:** Representative immunoblot showing changes in NCC phosphorylation at Thr 53 in response to changes in extracellular K^+ in kidney slices from control (upper panel) and CS-Kcnj10-KO mice (lower panel). Molecular weights indicated on the right in kDa **B:** Densitometric quantification of experimental series in A (n=6-9 slices from 3 mice per genotype). **p<0.01 assessed by unpaired Student's t-test). Mean ± SEM is represented In B.

Figure 3: Response of control and CS-Kcnj10-KO mice to treatment with hydrochlorothiazide (HCTZ) during three days (d1-d3) in metabolic cages. **A**: Urinary excretion of K^+ (upper graph), Na^+ (middle graph) normalized to creatinine and K^+/Na^+ ratio (lower graph) in CS-Kcnj10-KO mice treated with HCTZ. **B**: Same data as in A but normalized to control baseline (d0). *p<0.05; **p<0.01; ***p<0.001 assessed by unpaired Student's t-test. n=6 mice per genotype. In all graphs mean ± SEM is represented.

Figure 4: Response of control and CS-Kcnj10-KO mice to changes in dietary K^+. **A:** Urinary excretion of K^+ and Na^+ normalized to creatinine of control and CS-Kcnj10-KO mice subjected to low K^+ (LK) diet during three days in metabolic cages (n=6 mice per genotype). **B:** Urinary excretion of K^+ and Na^+ normalized to creatinine of control and CS-Kcnj10-KO mice subjected to high K^+ (HK) diet during three days in metabolic cages (n=6 per genotype). Statistical differences in all experiments were assessed by unpaired Student's t-test *p<0.05; **p<0.01; ***p<0.001. mean ± SEM is represented in graphs.

Figure 5: Characterization of control and CS-Kcnj10-KO mice on dietary K^+ deprivation. **A:** Immunoblot of the main ion channels and transporters expressed in the distal nephron of control and CS-Kcnj10-KO mice. (molecular weights indicated on the right in kDa) **B:** Densitometric analysis of immunoblots in A normalized to control (in red). **C:** Representative immunofluorescence staining of CSs from control and CS-Kcnj10-KO mice after three days on low K^+ diet. Consecutive sections were stained with αENaC (upper panel) and AQP2 antibodies (lower panel). Specific signal in red and background autofluorescence in green. **D:** Effect of a single i.p. dose of amiloride on urinary K^+ and Na^+ in control (n=6) and CS-Kcnj10-KO (n=5) mice after two days of dietary K^+ deprivation. Statistical differences assessed by two-way ANOVA with Tukey multiple comparison post-test (ns non-significant; *$p<0.05$, ***$p<0.001$).

Figure 6: Abundance of ROMK in control and CS-Kcnj10-KO mice and characterization of CS-Kcnj10-ROMK-KO mice. **A:** Representative immunofluorescent stainings in kidneys from control and CS-Kcnj10-KO mice after three days on low K^+ diet. Consecutive sections were stained with ROMK (upper panel) and AQP2 antibodies (lower panel). Specific signal in red and background autofluorescence in green. In the graph, the quantification of the staining intensity for ROMK across CS cells (basal – apical) from control (n=6) and CS-Kcnj10-KO (n=5) mice is represented. **B:** Concentration of K^+ in the plasma of control (n=9), CS-Kcnj10-KO (n=11) and CS-Kcnj10-ROMK-KO (n=8) mice after three days of dietary K^+ deprivation. Statistical differences assessed by one-way ANOVA with Tukey multiple comparison post-test (ns non-significant; **p<0.01). The data were averaged and are presented in Table 5. **C:** Effect of a single i.p. dose of amiloride on urinary K^+ and Na^+ in control and CS-Kcnj10-ROMK-KO mice after two days of dietary K^+ deprivation. n=9 mice per genotype. Statistical differences assessed by two-way ANOVA with Tukey multiple comparison post-test (ns non-significant; *p<0.05, **p<0.01).

Role of $Kir_{4.1}$ in the collecting system

Figure 7: Proposed model of the function of $Kir_{4.1}$ in the distal nephron in control conditions and in EAST/SeSAME syndrome.

Table 1: *Effect of Kcnj10 deletion in the collecting system on plasma parameters in mice under standard diet*

Parameter	control	CS-Kcnj10-KO
Na^+ (mmol/L)	147.0 ± 1.6	146.4 ± 1.2
K^+ (mmol/L)	3.4 ± 0.1	3.2 ± 0.1
Ca^{2+} (mmol/L)	0.9 ± 0.1	0.8 ± 0.1
Cl^- (mmol/L)	115.2 ± 2.1	113.6 ± 1.2
pH	7.3 ± 0.01	7.4 ± 0.02
HCO_3^- (mmol/L)	16.5 ± 0.4	16.6 ± 0.5
Hematocrit (%)	39.6 ± 1.2	39.0 ± 0.9

n=5 mice / group

Table 2: *Effect of Kcnj10 deletion in the CS on plasma parameters upon three days treatment with HCTZ*

Parameter	control	CS-Kcnj10-KO
Na^+ (mmol/L)	149.2 ± 0.5	145.2 ± 0.9[b]
K^+ (mmol/L)	3.7 ± 0.2	3.0 ± 0.1[a]
Ca^{2+} (mmol/L)	1.09 ± 0.05	0.94 ± 0.07
Cl^- (mmol/L)	105.2 ± 0.7	98.8 ± 0.7[d]
pH	7.37 ± 0.01	7.47 ± 0.01[d]
HCO_3^- (mmol/L)	19.9 ± 0.4	24.6 ± 0.4[d]
Hematocrit (%)	45.3 ± 0.6	47.8 ± 1.4

[a]p<0.05; [b]p<0.01; [d]p<0.0001 assessed by unpaired Student's t test. n=6 mice / group.

Table 3: *Effect of Kcnj10 deletion in the CS on plasma parameters in mice under low K^+ diet*

Parameter	control	CS-Kcnj10-KO
Na^+ (mmol/L)	151.0 ± 0.6	147.8 ± 1.4
K^+ (mmol/L)	3.1 ± 0.2	1.9 ± 0.1[c]
Ca^{2+} (mmol/L)	1.12 ± 0.06	0.99 ± 0.07
Cl^- (mmol/L)	113.6 ± 0.7	105.5 ± 1.2[c]
pH	7.31 ± 0.02	7.33 ± 0.02
HCO_3^- (mmol/L)	18.2 ± 0.7	21.5 ± 0.9[a]
Hematocrit (%)	43.2 ± 0.6	43.5 ± 0.7

[a]p<0.05; [c]p<0.001 assessed by unpaired Student's t test. n=6 mice / group.

Table 4: *Effect of Kcnj10 deletion in the CS on plasma parameters in mice under high K^+ diet*

Parameter	control	CS-Kcnj10-KO
Na^+ (mmol/L)	150.0 ± 1.0	150.0 ± 1.2
K^+ (mmol/L)	4.4 ± 0.2	4.1 ± 0.2
Ca^{2+} (mmol/L)	1.02 ± 0.07	0.98 ± 0.08
Cl^- (mmol/L)	113.3 ± 1.1	111.0 ± 1.1
pH	7.31 ± 0.02	7.34 ± 0.02
HCO_3^- (mmol/L)	18.4 ± 0.6	20.0 ± 0.5
Hematocrit (%)	44.8 ± 0.7	43.8 ± 0.9

n=6 mice / group.

Table 5: *Effect of Kcnj10 and Kcnj1 deletion in the CS on plasma parameters in mice under low K^+ diet*

Parameter	control (9)	CS-Kcnj10-KO (11)	CS-Kcnj10-ROMK-KO (8)
Na^+ (mmol/L)	151.2 ± 1.1	147.5 ± 1.2[a]	149.0 ± 0.5
K^+ (mmol/L)	2.6 ± 0.1	1.6 ± 0.1[d]	2.3 ± 0.1[****]
Ca^{2+} (mmol/L)	1.16 ± 0.06	1.14 ± 0.06	1.01 ± 0.05
Cl^- (mmol/L)	110.2 ± 1.0	102.9 ± 1.6[c]	106.1 ± 0.5
pH	7.26 ± 0.02	7.33 ± 0.02[a]	7.37 ± 0.02[c]
HCO_3^- (mmol/L)	17.1 ± 0.5	20.9 ± 0.7[c]	21.1 ± 0.6[c]
Hematocrit (%)	46.6 ± 1.0	43.0 ± 1.0[a]	39.5 ± 0.9[c*]

*[a]p<0.05; [b]p<0.01; [c]p<0.001; [d]p<0.0001; compared to control group assessed by one-way ANOVA with Tukey's multiple comparison post-test. *p<0.05; ****p<0.0001 compared to CS-Kcnj10-KO group assessed by one-way ANOVA with Tukey's multiple comparison post-test. Number of animals per group in parenthesis (n).*

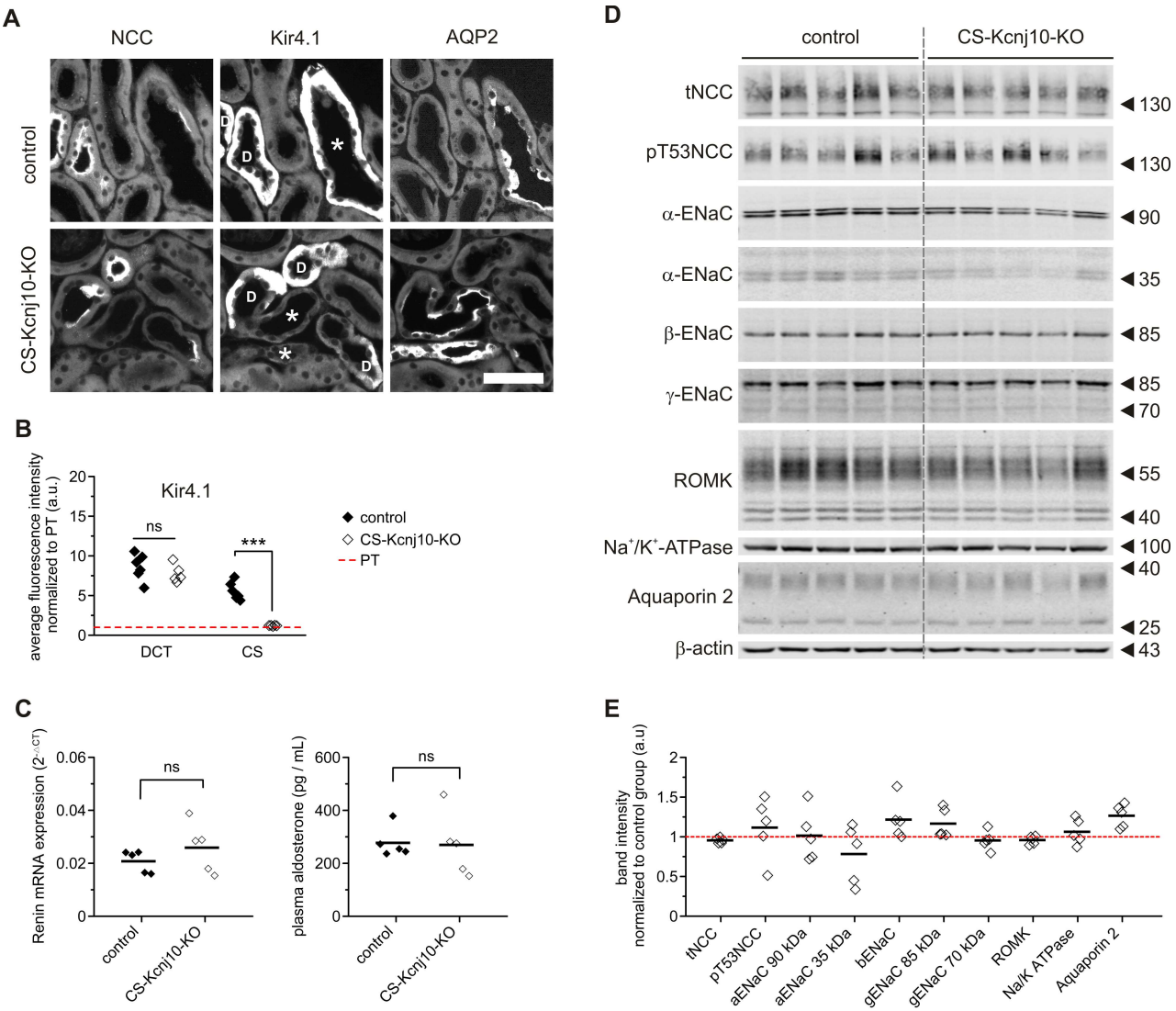
A
NCC
Kir4.1
AQP2
control
CS-Kcnj10-KO
D
B
Kir4.1
average fluorescence intensity normalized to PT (a.u.)
ns
***
control
CS-Kcnj10-KO
PT
DCT
CS
C
Renin mRNA expression (2^-ΔCT)
plasma aldosterone (pg / mL)
ns
control
CS-Kcnj10-KO
D
control
CS-Kcnj10-KO
tNCC
pT53NCC
α-ENaC
α-ENaC
β-ENaC
γ-ENaC
ROMK
Na+/K+-ATPase
Aquaporin 2
β-actin
130
130
90
35
85
85
70
55
40
100
40
25
43
E
band intensity normalized to control group (a.u)
tNCC
pT53NCC
aENaC 90 kDa
aENaC 35 kDa
bENaC
gENaC 85 kDa
gENaC 70 kDa
ROMK
Na/K ATPase
Aquaporin 2

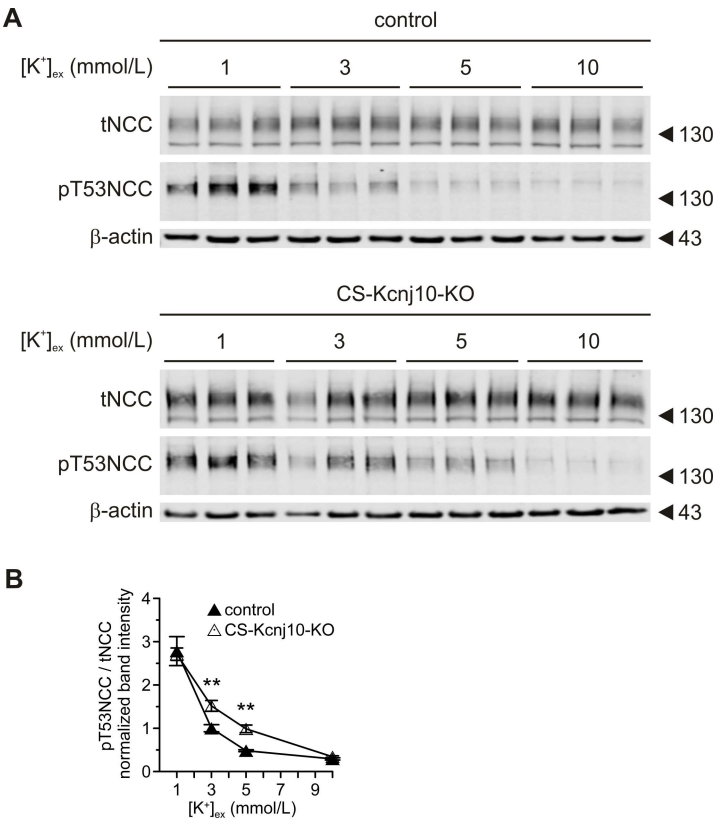
A
control
[K+]ex (mmol/L)
1
3
5
10
tNCC
pT53NCC
β-actin
130
130
43
CS-Kcnj10-KO
[K+]ex (mmol/L)
1
3
5
10
tNCC
pT53NCC
β-actin
130
130
43
B
control
CS-Kcnj10-KO
pT53NCC / tNCC
normalized band intensity
**
**
[K+]ex (mmol/L)

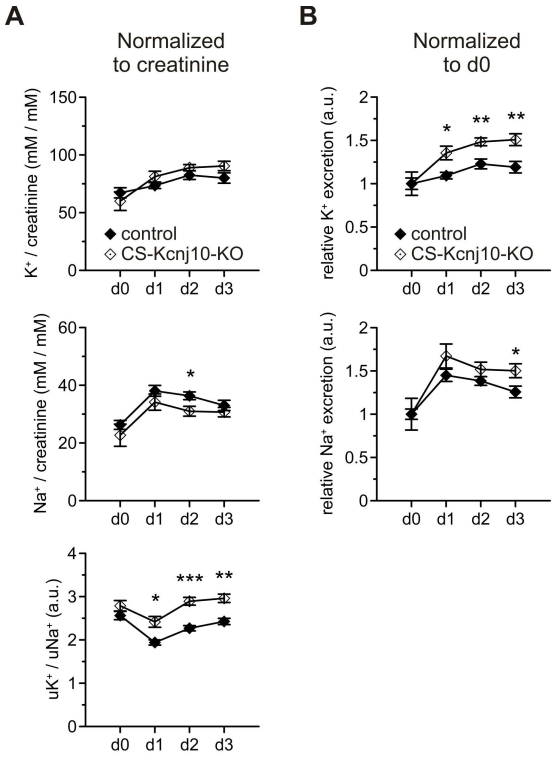
A
Normalized
to creatinine
K+ / creatinine (mM / mM)
150
100
50
0
control
CS-Kcnj10-KO
d0 d1 d2 d3
Na+ / creatinine (mM / mM)
60
40
20
0
*
d0 d1 d2 d3
uK+ / uNa+ (a.u.)
4
3
2
1
0
*
***
**
d0 d1 d2 d3
B
Normalized
to d0
relative K+ excretion (a.u.)
2
1.5
1
0.5
0
*
**
**
control
CS-Kcnj10-KO
d0 d1 d2 d3
relative Na+ excretion (a.u.)
2
1.5
1
0.5
0
*
d0 d1 d2 d3

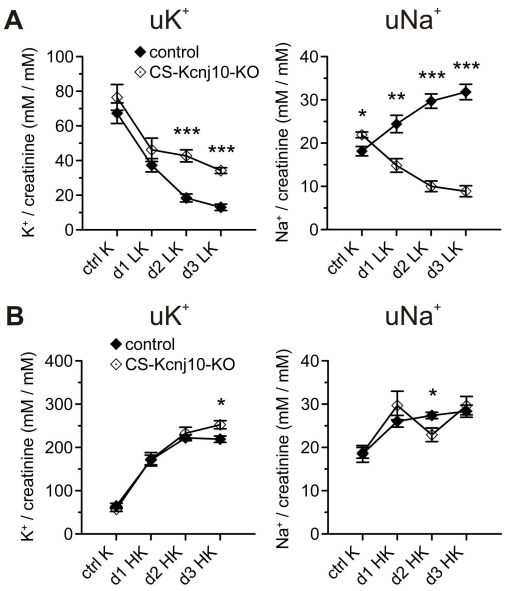
A
uK+
uNa+
control
CS-Kcnj10-KO
K+ / creatinine (mM / mM)
Na+ / creatinine (mM / mM)
ctrl K
d1 LK
d2 LK
d3 LK
B
uK+
uNa+
control
CS-Kcnj10-KO
K+ / creatinine (mM / mM)
Na+ / creatinine (mM / mM)
ctrl K
d1 HK
d2 HK
d3 HK

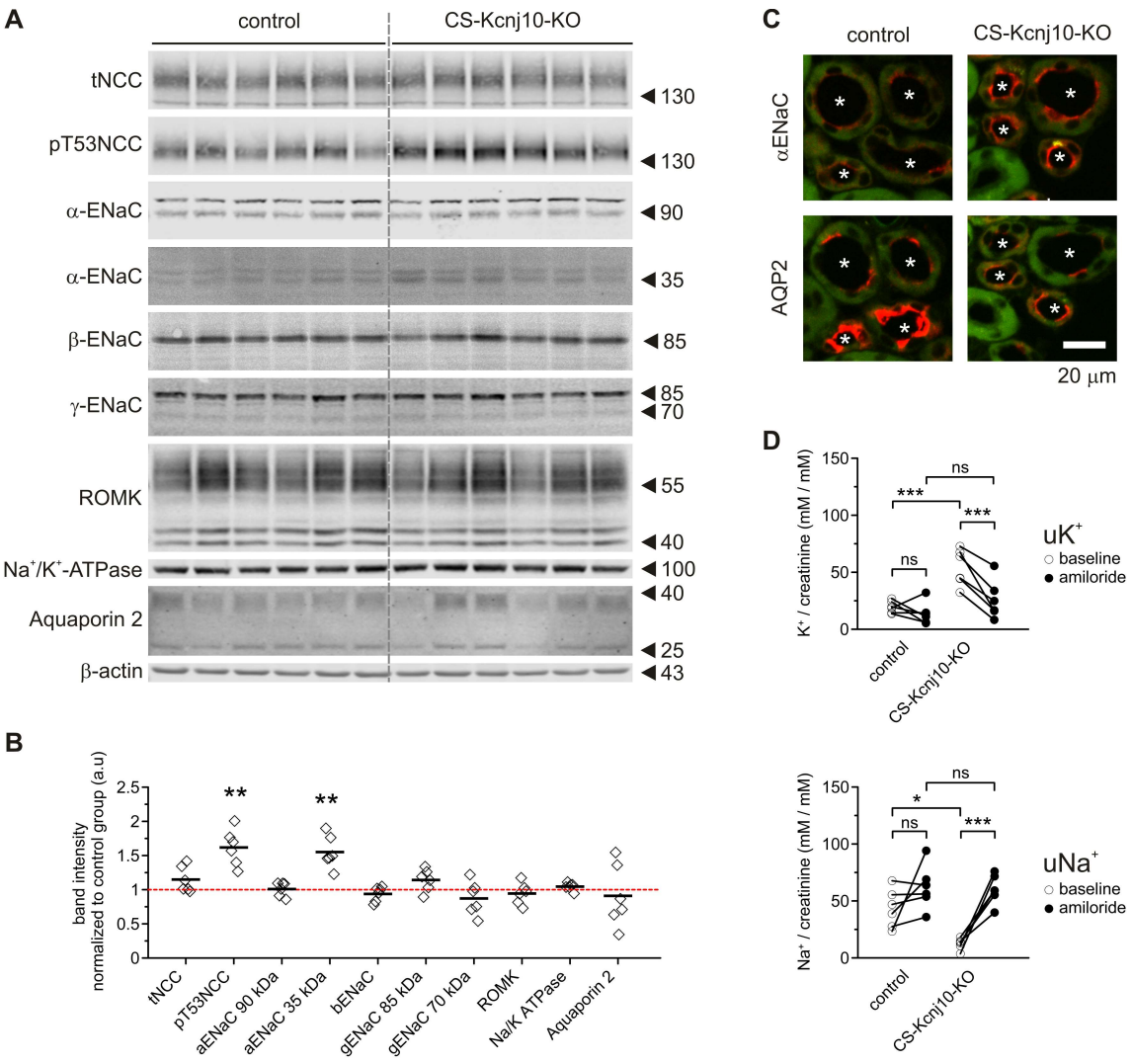
A
control
CS-Kcnj10-KO
tNCC
pT53NCC
α-ENaC
α-ENaC
β-ENaC
γ-ENaC
ROMK
Na+/K+-ATPase
Aquaporin 2
β-actin
130
130
90
35
85
85
70
55
40
100
40
25
43
B
band intensity
normalized to control group (a.u)
2.5
2
1.5
1
0.5
0
**
**
tNCC
pT53NCC
aENaC 90 kDa
aENaC 35 kDa
bENaC
gENaC 85 kDa
gENaC 70 kDa
ROMK
Na/K ATPase
Aquaporin 2
C
control
CS-Kcnj10-KO
αENaC
AQP2
20 μm
D
K+ / creatinine (mM / mM)
150
100
50
0
ns
***
***
ns
control
CS-Kcnj10-KO
uK+
baseline
amiloride
Na+ / creatinine (mM / mM)
150
100
50
0
ns
*
ns
***
control
CS-Kcnj10-KO
uNa+
baseline
amiloride

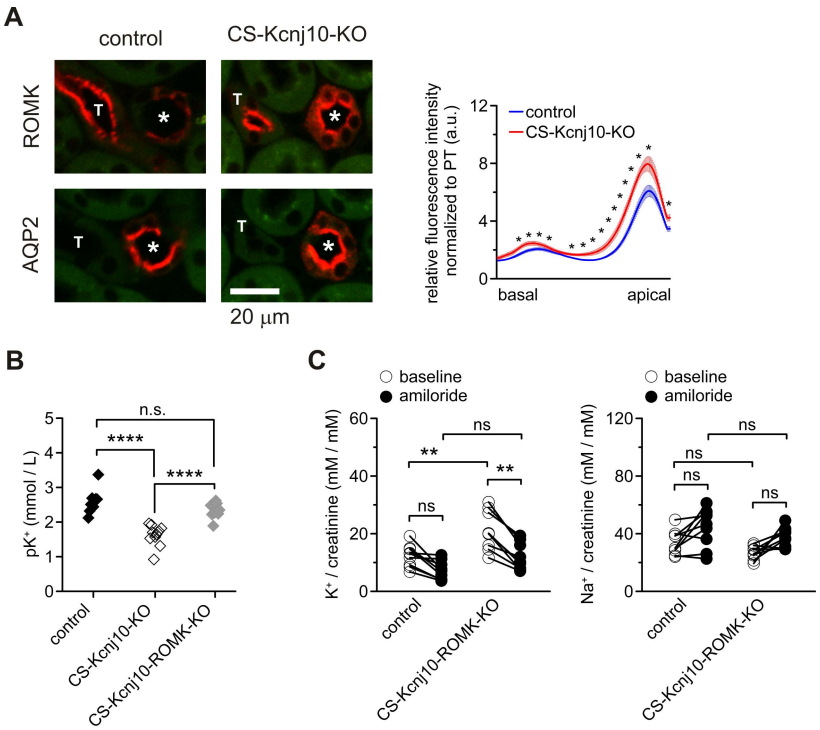
A
control
CS-Kcnj10-KO
ROMK
AQP2
T
*
20 μm
relative fluorescence intensity normalized to PT (a.u.)
control
CS-Kcnj10-KO
basal
apical
B
pK+ (mmol / L)
n.s.
****
control
CS-Kcnj10-KO
CS-Kcnj10-ROMK-KO
C
baseline
amiloride
K+ / creatinine (mM / mM)
Na+ / creatinine (mM / mM)
ns
**
control
CS-Kcnj10-ROMK-KO

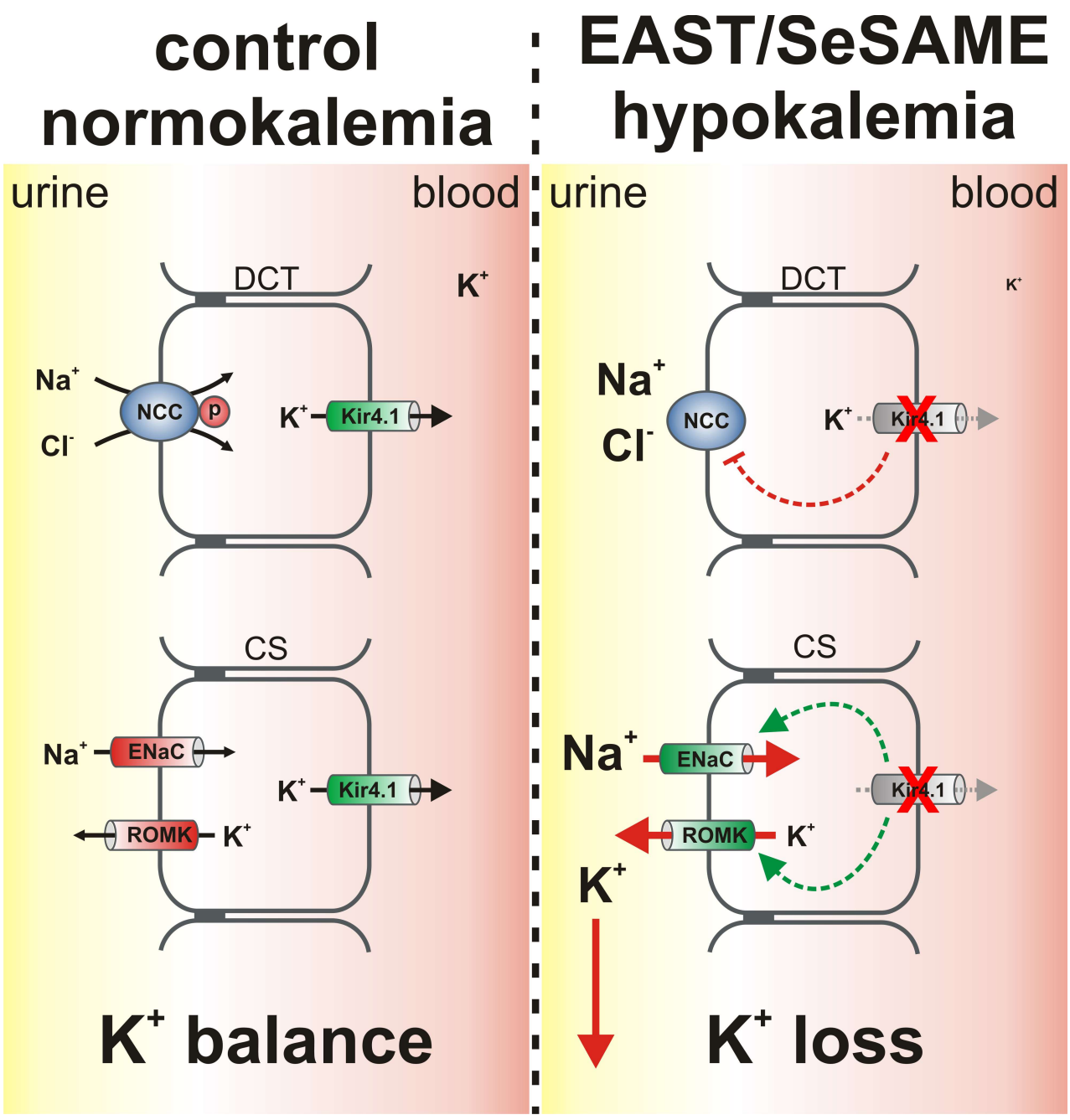
control
normokalemia
EAST/SeSAME
hypokalemia
urine
blood
DCT
K+
Na+
Cl-
NCC
P
K+
Kir4.1
CS
Na+
ENaC
K+
Kir4.1
ROMK
K+
K+ balance
urine
blood
DCT
K+
Na+
Cl-
NCC
K+
Kir4.1
CS
Na+
ENaC
Kir4.1
ROMK
K+
K+
K+ loss

Supplementary Material Table of Contents

Supplementary methods

ROMK antibody

A novel rabbit anti-ROMK antibody recognizing the C-terminal region of ROMK was custom made by Pineda Antikörper-Service (Berlin, Germany). After immunization of rabbits against the peptide NH2-CDNPNFVLSEVDETDDTQM-CCOH, the obtained antisera were affinity-purified against the immunizing peptide. As shown in Supplementary Fig. 3, the antibody shows a similar banding pattern on immunoblots of mouse kidneys as previously observed by Wade and co-workers[1] using a different anti-ROMK antibody (IB: 1: 2000). Moreover, immunostaining of kidney from CS-Kcnj10-ROMK-KO confirmed the specificity of the ROMK antibody (IF: 1: 12000). While a strong ROMK-related immunostaining was seen in non-targeted DCT cells, no immunofluorescent signal was seen in connecting tubules and collecting ducts, in which ROMK was deleted (Supplementary Fig. 2).

Sample preparation for quantitative qPCR

Kidneys were removed and immediately transferred into RNA lysis buffer and homogenized using Percellys Tissue Homogenizer (Bertin Technologies SAS, Montigny-le-Bretonneux, France). RNA was isolated using the NucleoSpin® kit (Macherey-Nagel GmbH, Düren, Germany) as per the manufacturer`s protocol. 1 µg of total RNA was used to generate cDNA using the kit GoScript Reverse Transcription System (Promega AG, Dübendorf, Switzerland) as per the protocol. The cDNA was diluted 1:5 with nuclease-free water for qRT-PCR.

Primers

The following primers were used for quantitative PCR (qPCR) and genotyping:

Primer name	Sequence	Use
Kcnj10 flox	Fwd: ATCTCGATTGCTGCTTGAGA Bckwd: TTTTGCCCTACTCAATGCTCT	Genotyping
Aqp2Cre	Fwd1: AAGTGCCCACAGTCTAGCCTCT Fwd2: CCTGTTGTTCAGCTTGCACCAG Bckwd: GGAGAACGCTATGGACCGGAGT	
ROMK flox	Fwd: GTGCCATGTGCCTCTATAATGAGA Bckwd: TCTTCTAGAATCATAGCCATGGGG	
renin	Fwd: GGAGGAAGTGTTCTCTGTCTACTACA Bckwd: GCTACCTCCTAGCACCACCTC	qPCR
β-actin	Fwd: CCACCGATCCACACAGAGTACTT Bckwd: GACAGGATGCAGAAGGAGATTACTG	

Immunofluorescence (IF) and IF quantification

For IF quantification, images were acquired using a spinning disc confocal microscope (Olympus IX83) equipped with a 30X UPLSAPO UPlan S Apo silicon oil immersion objective. To this end, 6 control and 5 CS-Kcnj10-KO mice were subjected to dietary K^+ deprivation for 3 days and perfused with 3% PFA. Consecutive cryosections of perfusion-fixed kidneys were stained with rabbit polyclonal antibodies against NCC (labeling the DCT) and / or AQP2 (labeling CNT and CD) and one of the proteins of interest (i.e. αENaC, ROMK, or $Kir_{4.1}$). Sections were then imaged at a confocal microscope by an investigator blinded for the genotype of the analyzed mice. Subsequently, obtained images were independently analyzed by two investigators without knowledge of the genotype of the mice. Both investigators came to the same conclusions regarding the expression levels and the subcellular localization of the studied proteins in the respective mice. To confirm the qualitative judgements of the two investigators, ROMK and $Kir_{4.1}$, staining intensities were also quantified using imaging software (see below).

For the quantification of $Kir_{4.1}$, three cryosections per animal (6 control mice and 5 CS-Kcnj10-KO mice) were imaged and the mean fluorescence intensity was measured in 5 proximal tubule (PTs), 10 DCTs and 10 CS per section as depicted in supplementary Fig. 4A using the ImageJ software. The mean fluorescence intensity of each structure was normalized to the mean intensity of all PTs of the same section to obtain its relative fluorescence intensity (RFI) per section. The RFI obtained for each section was then again averaged to serve as average value for each animal data to calculate the mean values for each of the two animal groups.

For the quantification of ROMK, the axial fluorescence intensity (basal to apical) was measured in 5 proximal tubule (PTs) cells and 10 CS cells as depicted in supplementary Fig. 4B using the ImageJ software and the provided supplementary macro. The axial fluorescence intensity of each CS cell was normalized to the mean axial intensity of the PTs of the same section to obtain the CS relative axial fluorescence intensity (CS-RAFI) of this cell. All 10 CS-RAFI from each image were averaged to obtain the section CS-RAFI, while section CS-RAFI obtained from each animal were averaged to obtain the CS-RAFI corresponding to each animal. Finally, the CS-RAFI corresponding to 6 control animals and 5 CS-Kcnj10-KO mice are represented in Figure 6 as mean ± SEM.

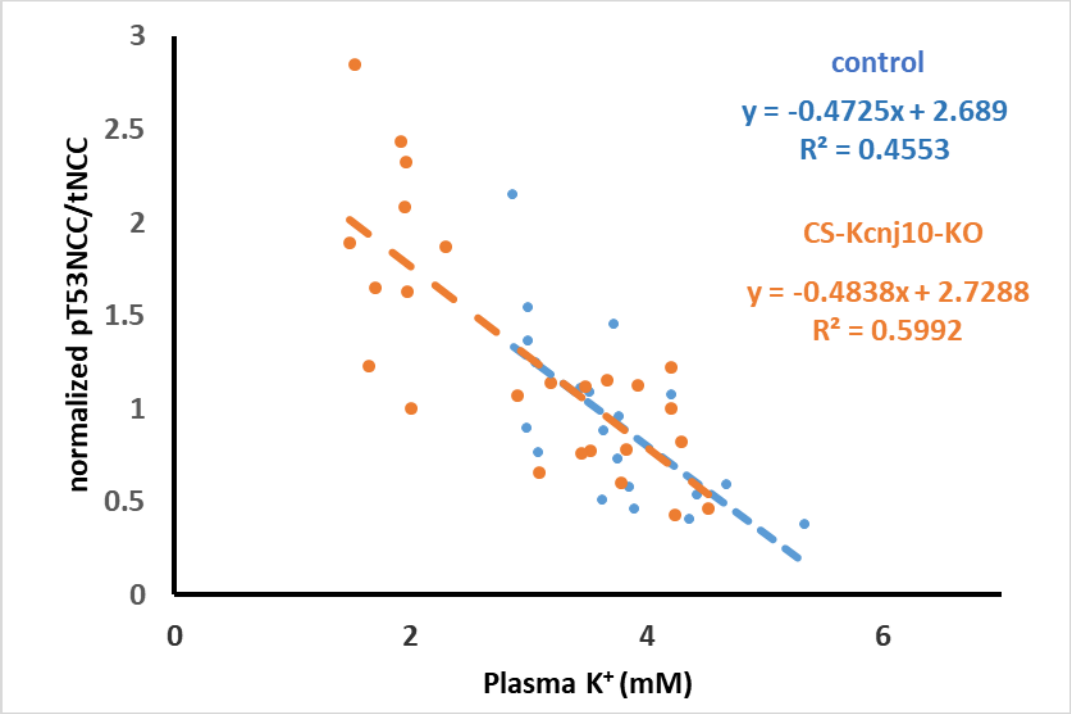

Supplementary Figure 1: Correlation of NCC phosphorylation with plasma K^+ concentration in control (n=20) and CS-Kcnj10-KO (n=25) mice.

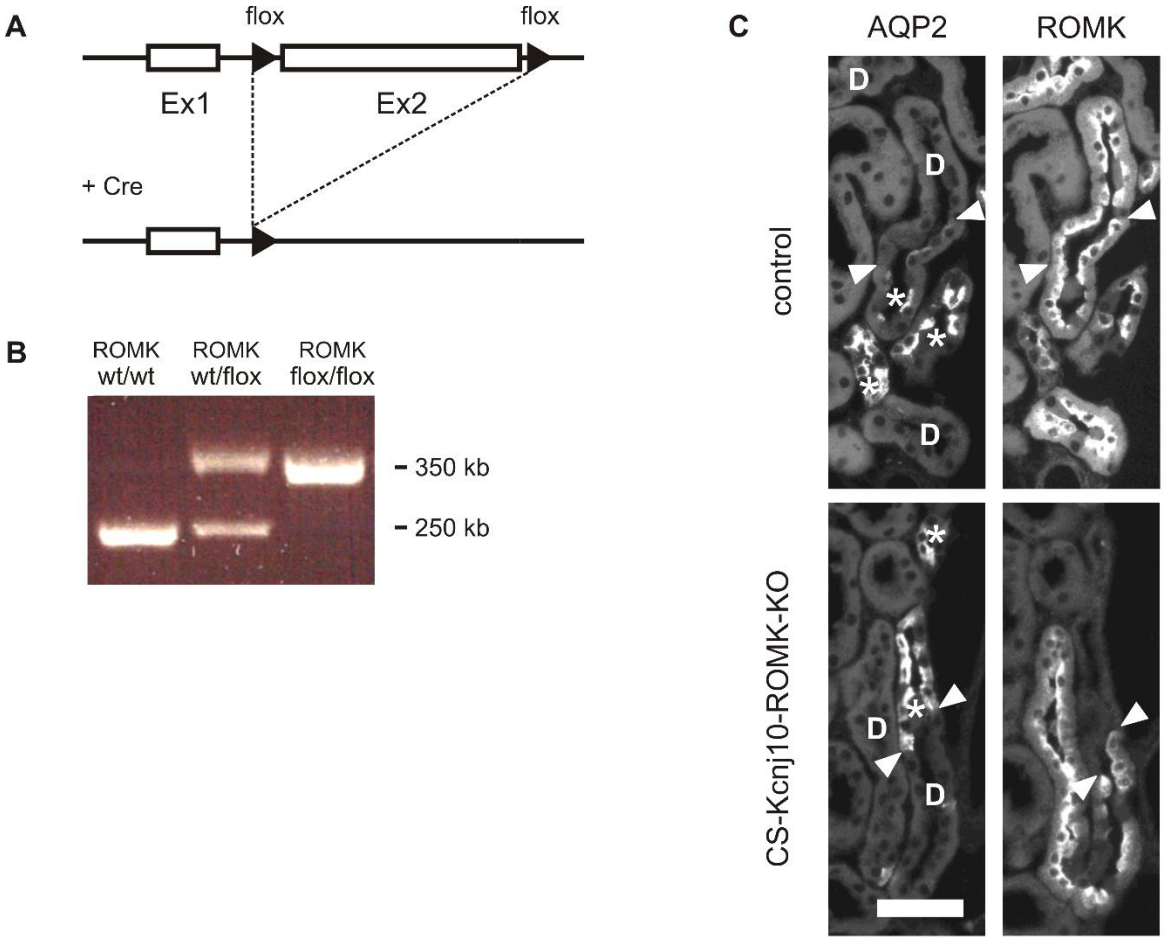

Supplementary Figure 2: Characterization of CS-Kcnj10-ROMK-KO mouse model. **A:** Scheme of genetic modification of Kcnj1$^{flox/flox}$ mice before and after cre-mediated recombination. **B:** Genotyping of Kcnj1$^{flox/flox}$ mice. **C:** Immunofluorescence staining of AQP2 and ROMK in consecutive sections from kidneys of control and CS-Kcnj10-ROMK-KO mice. DCTs are labeled with a D while CSs are labelled with a star. Transitions DCT-CNT are marked with arrowheads. Scale bar 50 μm.

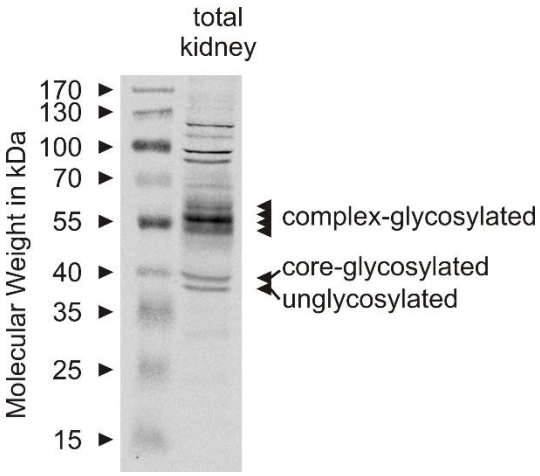

Supplementary Figure 3: Characterization of novel rabbit anti-ROMK antibody using lysates of total kidneys of control mice. Bands were identified and labelled according to Wade et al[1].

A

Kir4.1

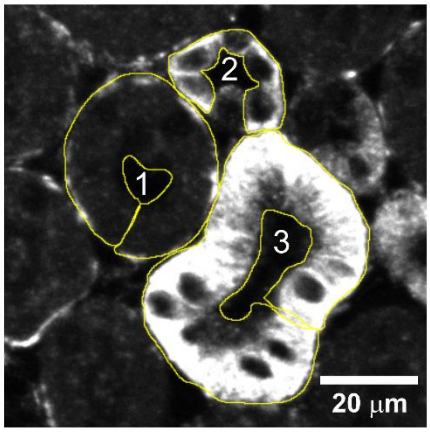

segment	average fluorescence intensity (a.u.)
PT (1)	9600.22
CS (2)	28385.81
DCT1 (3)	45237.23

B

ROMK

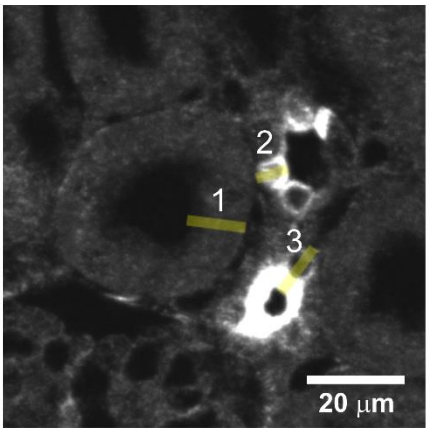

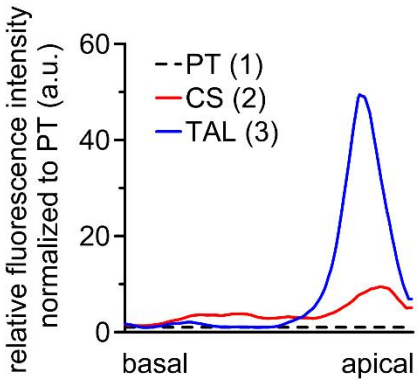

Supplementary Figure 4: Examples of Immunofluorescence quantification.

A: Quantification of fluorescence intensity of ROMK staining across cells (basal – apical) in cells of the PT (1), CS (2) and TAL (3). In the graph, the relative fluorescence intensity is normalized to PT fluorescence. **B:** Quantification of average fluorescence intensity of $Kir_{4.1}$ staining in a PT (1) CS (2) and DCT (3).

Supplementary Table 1: *Effect of Kcnj10 and ROMK deletion in the collecting system on plasma parameters in mice under standard diet.*

Parameter	control	CS-Kcnj10-ROMK-KO
Na^+ (mmol/L)	148.0 ± 0.3	148.8 ± 0.8
K^+ (mmol/L)	3.3 ± 0.1	3.2 ± 0.2
Ca^{2+} (mmol/L)	1.0 ± 0.04	1.1 ± 0.03[a]
Cl^- (mmol/L)	108.7 ± 0.8	109.4 ± 1.3
pH	7.2 ± 0.02	7.3 ± 0.03
HCO_3^- (mmol/L)	17.4 ± 0.5	18.3 ± 0.6
Hematocrit (%)	43.2 ± 1.1	42.0 ± 1.9

[a]p<0.05 assessed by unpaired Student's t test. n=5 mice / group.

Supplementary Macro

```
/*
* Normalizes line profiles by making use of the Straighten command followed by scaling
* By Olivier Burri, BioImaging And Optics Platform
* In Response to http://forum.imagej.net/t/average-pixels-with-line-tool/6408?u=oburri
* Modified by Joana R. Martins, Center of Microscopy and Image Analysis, University of Zurich
* OUTPUT is the values of the line profile as a results table
* Column name is the image name.
* the number of rows corresponds to the normalization length normLength
*/
//setBatchMode(true);
normLength = 200; //px the final length you want
lineWidth = 10; // Line thickness to average intensities along the perpendicular axis
imageName = getTitle();
print("image name is "+imageName);
nROIs = roiManager("count");
print(nROIs);
for (j = 0; j < nROIs ; j++) {
selectWindow(imageName);
roiManager("select", j);
print("loop" + j);
run("Straighten...", "title=SubImage line="+lineWidth);
run("Scale...", "x=- y=- width="+normLength+" height="+lineWidth+" interpolation=Bilinear create");
```

```
run("Line Width...", "line="+lineWidth);
makeLine(0,lineWidth/2, normLength, lineWidth/2);
data = getProfile();
for(i=0; i<normLength; i++) {
setResult(j, i, data[i]);
}
close();
close();
}
//setBatchMode(false);
```

References

1. Wade JB, Fang L, Coleman R a, Liu J, Grimm PR, Wang T, Welling P a: Differential regulation of ROMK (Kir1.1) in distal nephron segments by dietary potassium. *Am. J. Physiol. Renal Physiol.* 300: F1385-93, 2011